

Optoelectronic Properties Enhanced by Photodynamic Patterning of Azo Polymers

Dong-Yu Kim*

Center for Frontier Materials, Heeger Center for Advanced Materials (HCAM), Department of Materials and Engineering, Gwangju Institute of Science and Engineering (GIST), Gwangju, Korea
kimdy@gist.ac.kr

Introduction

Azobenzene functionalized polymers have been extensively investigated due to the potential applications in the areas of optical switching, optical elements, optical information storage, and nonlinear optics.¹ These applications are mainly achievable due to photoinduced properties of azobenzene groups with photoisomerization and photoinduced anisotropy. Azobenzene groups experiences a reversible *trans-cis-trans* isomerization and an orientational distribution perpendicular to the direction of the polarization of the incident light beam when a polarized light beam at a proper wavelength is irradiated. Especially, a continuous isomerization cycling initiates an unusual mass transport process. Surface relief gratings (SRGs) are formed on azo polymer films at temperature below the glass transition as interferometric beam pattern is illuminated.^{2,4} The modulation depth of inscribed SRGs is strongly dependent on the photo exposure time, the state of polarization of the writing beam, the chemical structure of azo materials. This process can provide various advantages such as capability to superimpose multiple patterns, to directly inscribe patterns, as well as flexibility control of the modulation period and depth.

We report applications to the optoelectronic devices using inscribed one- (1D) and two-dimensional (2D) SRGs on azo polymer films. The inscribed holographic SRGs patterns were useful to control or enhance optoelectronic properties.

Experimental

The utilized SRGs for applications referred on this paper were mainly obtained by the following process. Azo polymers were dissolved in cyclohexanone and a filtered 10 wt % azo polymer solution was spin coated on glass slides or silicon wafer. Fabricated films were baked under vacuum at around 70 °C for 5 h. Holographic SRGs were fabricated on the films coated with azo polymers using an interference pattern of an Ar ion laser beam at 488 nm as shown in Fig. 1. The intensity of the laser beam was 100 mW/cm². The linearly polarized light of the Ar ion laser beam was passed through a half waveplate to set a p-polarized state. It was then expanded and collimated through a spatial filter and a lens. About half of the collimated beam was directly incident on the film and the other part was reflected on the film by an aluminium-coated mirror. The polarization of the writing beam was p-polarization with respect to the film plane and the incident angle of the writing beam was controlled to fabricate 350 nm ~ several μm grating spacing according to Bragg's law ($\lambda = 2d \sin \theta$, where λ = wavelength, d = period of interference pattern, θ = incident angle). Surface images and depth profiles of the photo-fabricated SRGs were measured by atomic force microscopy (AFM). Fig. 2 shows various SRGs images. Fig. 2(a) is the normal 1D SRGs after the single exposure of interference beams. Fig. 2(b) shows two sets of gratings like egg-crate recorded orthogonally to each other. Fig. 2(c) shows a Fourier blazed grating.

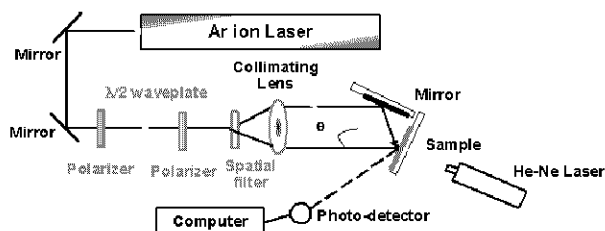


Figure 1. Set-up for holographic SRG formation

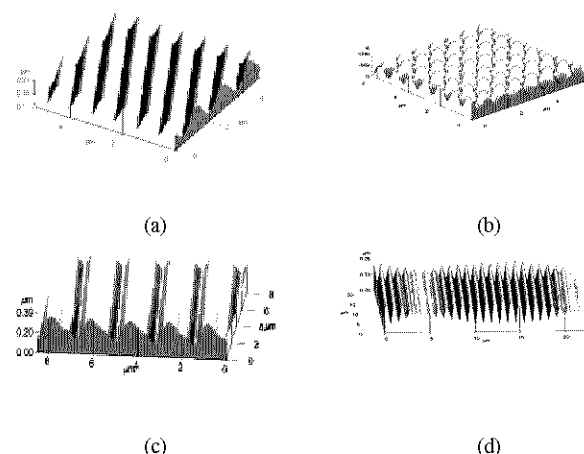


Figure 2. AFM images of various SRGs

Fig. 2(d) shows a typical beat structures recorded sequentially with two wavelengths at 488 nm and 514 nm at a fixed writing angle. The formation of SRGs was confirmed by monitoring of the first-order diffraction from a 1.2 mW He-Ne laser beam at 633 nm in the transmission mode.

Results and discussion

TiO₂ nanostructures fabricated using surface relief gratings.

Well-ordered TiO₂ nanostructures such as 1-dimensional nanowire arrays, 2-dimensional square and hexagonal hole arrays, and 3-dimensional wire junction arrays were fabricated by a simple, controllable, economical, and reproducible method using surface relief gratings on azobenzene-functionalized polymer films as a template in the sol-gel reaction of a Ti precursor. In addition, as an application of TiO₂ nanostructure, transparent electrodes were patterned by selective dry etching with the TiO₂ nanowire array etch mask.⁵

Fig. 3 shows atomic force microscopy (AFM) images of 1D and 2D SRGs which are fabricated on the polymer film. Using the one-step illumination process and superposition of two sets of gratings orthogonal with respect to each other, 1D and 2D orthogonal cross grating patterns were obtained on the polymer films as shown in Fig. 3(a) and (b), respectively. To produce the hexagonal 2D SRG shown in Fig. 3(c), the substrate with a 1D SRG was rotated by 60° around its normal axis followed by a second exposure. Here, the spacing and depth of the SRGs can be easily controlled by the incident angle of the interfering laser beams and the irradiation time, respectively.

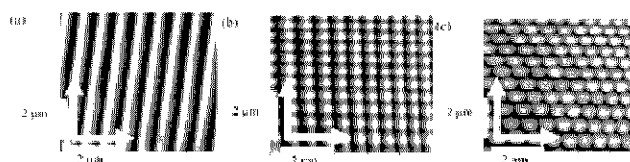


Figure 3. AFM images of (a) 1D SRGs on a polymer film, (b) 2D square SRGs on a polymer film, and (c) 2D hexagonal SRGs on a polymer film

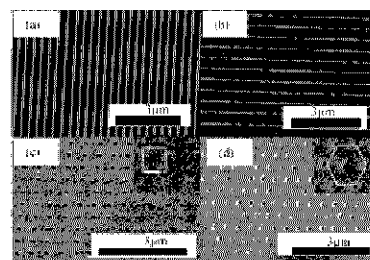


Figure 4. SEM images of (a) a TiO₂ nanowire array on ITO, (b) a 3D TiO₂ nanowire junction array on ITO by the repeated fabrication process of TiO₂ nanowire arrays, and 2D TiO₂ nanostructures with (c) a square array of periodic holes, and (d) a hexagonal array of periodic holes on ITO using 2D SRGs as templates.

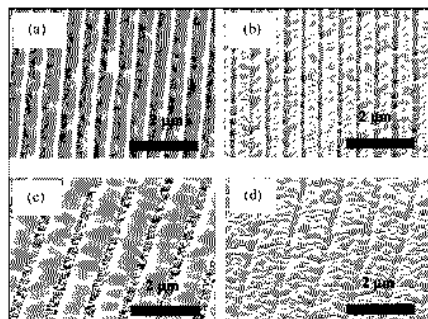


Figure 5. SEM images of (a) a TiO₂ nanowire etch mask on FTO using SRGs with a spacing of 500 nm, (b) a patterned FTO with (a) as an etch mask, (c) TiO₂ nanowire etch mask on FTO using SRGs with a spacing of 1000 nm, and (d) a patterned FTO with (c) as an etch mask.

Transparent electrode patterning using TiO₂ nanostructures.

A variety of SRG patterns as shown in Fig. 3 fabricated by controlling the rotation angle of the sample at the second exposure process were used as template for TiO₂ nanostructures. During the spin-on based sol-gel reaction with the 1D SRG as a template, Ti precursor underwent the sol-gel reaction and changed into TiO₂ nanowire structures formed along the grooves on the 1D SRGs. Finally, well-ordered TiO₂ nanowire arrays on the substrate were obtained as a result of the sintering to remove the polymer film and crystallize TiO₂ as shown in Fig. 4. It is clearly shown that the uniformity and order of the wire array have been significantly improved without acid treatment in the Ti precursor solution. Fig. 4(b), 4(c) and 4(d) show 3D TiO₂ wire junction arrays, square hole arrays and the hexagonal arrays of holes, respectively as the result of the repeated superposition process.

TiO₂ nanowire etch masks fabricated using SRGs on a polymer with spacings of 500 nm and 1000 nm were applied to patterning the FTO. Tilted SEM images of the TiO₂ nanowire etch mask on FTO and final well-patterned FTO are shown in Fig. 5. As shown in Fig. 5(a) and (b), the width of the TiO₂ nanowire etch mask and the feature size of patterned FTO was estimated to be 350 nm and 140 nm, respectively, when the SRG with a spacing of 500 nm was used as the template. When the spacing of the SRGs on the polymer film was increased to 1000 nm, a TiO₂ nanowire etch mask with a width of 770 nm was formed and the FTO was well-patterned with a feature size of 230 nm as shown in Fig. 5(c) and (d). Although the surface morphology of the FTO is rougher (>15 nm) than that of the ITO (~3 nm), the patterning of the FTO was successful as well, as shown in Fig. 5.

Efficient hybrid solar cells with ordered TiO₂ and conjugated polymer. The fabrication of ordered heterojunction organic-inorganic hybrid solar cells using well-ordered nanostructures of TiO₂ and MEH-PPV as an electron acceptor and donor, respectively, are described. The well-ordered TiO₂ nanostructure which has periodic hexagonal hole arrays of ~90 nm was fabricated using 2D surface relief gratings on azobenzene-functionalized polymer films as templates in the sol-gel reaction of a Ti-precursor. The efficiency was increased from 0.05 % and 0.12 %, for the flat TiO₂ film and random network of TiO₂ nanoparticles, respectively, and was further increased to 0.21 % using ordered 2D TiO₂ nanostructures due to the relatively high interfacial area and the efficient charge separation and charge transport as shown in Fig. 6.

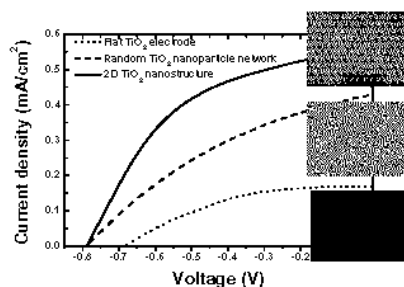


Figure 6. I-V curves of hybrid solar cell with three types of TiO₂ acceptor layers.

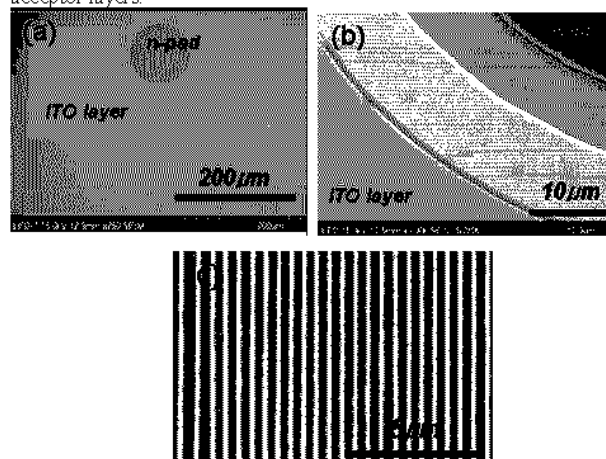


Figure 7. (a) A top-view SEM image of the 1D nanopatterned LED structure. (b) and (c) Enlarged images.

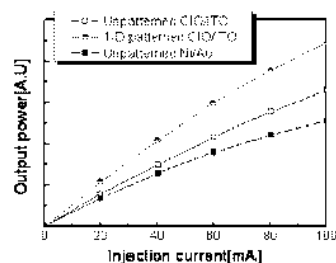


Figure 8. The *L-I* characteristics of LEDs fabricated with the 1D nanopatterned ClO/ITO, unpatterned ClO/ITO, and conventional Ni/Au contacts as a function of the forward drive current

Enhancement of the light output of GaN-based ultraviolet light-emitting diodes. The enhancement of the output power of ultraviolet GaN-based light-emitting diodes (LEDs) was observed by using one-dimensionally nanopatterned Cu-doped indium oxide (ClO)/indium tin oxide (ITO) *p*-type contact layers.⁶ The one-dimensional 1D nanopatterns (250 nm in width and 100 nm in depth) are defined using a TiO₂ 1D nanomask fabricated by means of a surface relief grating technique as shown in fig 7. When fabricated with the nanopatterned *p*-contact layers, the output power of LEDs is improved by 40 and 63% at 20 mA as compared to those fabricated with the unpatterned ClO/ITO and conventional Ni/Au contacts, respectively as shown in Fig. 8.

Conclusions

We have successfully demonstrated various applications of SRGs on azo polymer films to optoelectronic devices such as transparent electrode patterning, hybrid solar cell and ultraviolet GaN-based LED. Compared with the conventional method of patterning, this process showed significant advantages such as a one step process, controllability of the grating profiles, reversibility, and ability to form various structures due to the superimposability.

References

- [1] Natansohn, A. and Rochon, P. *Adv. Mat.* **1999**, *11*, 1387.
- [2] Rochon, P., Batalla, E., and Natansohn, A. *Appl. Phys. Lett.* **1995**, *66*, 136.
- [3] Pedersen, T. G., Johansen, P. M., Holme, N. C. R., and Ramanujam, P. S. *Phys. Rev. Lett.*, **1998**, *80*, 89.
- [4] Kim, D. Y., Tripathy, S. K., Li, L., and Kumar, J. *Appl. Phys. Lett.* **1995**, *66*, 1166.
- [5] Kim, S.-S., Chun, C., Hong, J.-C., and Kim, D.-Y. *J. Mater. Chem.* **2006**, *16*, 370.
- [6] Hong, H. G., Kim, S.-S., Kim, D.-Y., Lee, T., Song, J.-O., Cho, J. H., Sone, C., and Park, Y., Seong, T.-Y. *Appl. Phys. Lett.* **2006**, *88*, 103505.